Journal of Magnetic Resonance **152,** 227–233 (2001)
doi:10.1006/jmre.2001.2410, available online at http://www.idealibrary.com on IDEAL®

The Effect of RF Inhomogeneity on Heteronuclear Dipolar Recoupling in Solid State NMR: Practical Performance of SFAM and REDOR

Katsuyuki Nishimura,* Riqiang Fu,* and Timothy A. Cross*,†,[1]

*Center for Interdisciplinary Magnetic Resonance at the National High Magnetic Field Laboratory, 1800 E. Paul Dirac Drive, Tallahassee, Florida 32310; and †Department of Chemistry and Institute of Molecular Biophysics, Florida State University, Tallahassee, Florida 32310

Received February 15, 2001; revised July 10, 2001; published online September 4, 2001

Practical heteronuclear dipolar recoupling performances under magic angle spinning for SFAM and REDOR have been investigated under well-defined rf inhomogeneity environments with variation of resonance offsets for the irradiated nucleus. The heteronuclear dipolar recoupling efficiencies were quantitatively determined based on the experimentally obtained rf homogeneity. As a result, SFAM retains higher recoupling efficiency (>95%) at an 85% effective nutation frequency, and its recoupling efficiency is gradually reduced at lower effective nutation frequencies. On the other hand, although REDOR retains higher recoupling (>95%) efficiency at high (>92%) effective nutation frequency with an XY-8 compensation pulse sequence, the recoupling efficiency is dramatically decreased when the effective nutation frequency is below 90%. Over all, SFAM has significant advantages for insensitivity to carrier frequency offset and rf inhomogeneity.

Key Words: **solid state NMR; rf inhomogeneity; dipolar recoupling; SFAM; REDOR.**

INTRODUCTION

Interatomic distances represent one of the important restraint types for characterizing macromolecular structure. In solid state NMR experiments, relatively long interatomic distances can be obtained precisely and accurately through hetero- (*1–4*) and homonuclear (*5–10*) dipolar interactions. However, many of these solid state NMR experiments are strongly dependent on the precise setting of pulse lengths and phases as well as on exact rotor synchronization. Consequently, they become very sensitive to the deviation and fluctuation of experimental parameters. In addition, many important biomolecules have low sensitivity due to the small fraction of a mole in the sample. Unfortunately dipolar recoupling methods are also sensitive to rf inhomogeneity as reported previously (*11*, *12*). As a result, the observed dipolar coupling is not measured accurately, indeed it is generally underestimated resulting in the determination of longer interatomic distances.

Recently, a new generation experiment has been developed, in which phase and amplitude are simultaneously modulated, known as "simultaneous frequency and amplitude modulation (SFAM)" (*2*) to recouple the heteronuclear dipolar interaction under magic angle spinning (MAS) conditions. This method seems to be relatively insensitive to the carrier offset and to the variation of several experimental parameters without pulse compensation schemes. These features greatly benefit biological sample experiments as mentioned above.

In the well-known and established rotational echo double resonance (REDOR) (*1*) experiment, the heteronuclear dipolar Hamiltonian is inverted by a π pulse in the middle of each rotor period to cancel out the sign change of the Hamiltonian resulting from the sample rotation, thus preventing the dipolar interaction from being averaged by MAS. Another π pulse is applied in the end of each rotor period so that the recoupled heteronuclear dipolar interaction can be accumulated from one rotor period to the next one. As a result, the toggling function of the heteronuclear dipolar Hamiltonian for REDOR becomes a rectangular function, which is sensitive to the flip angle error of the π pulses. Without a compensation scheme the flip angle error may accumulate and thus cause a serious reduction in the recoupling efficiency for heteronuclear dipolar interactions. On the other hand, in the SFAM experiment, because of the continuous amplitude and phase modulated rf irradiation, the toggling function of heteronuclear dipolar Hamiltonian becomes a cosine function, except for the two π pulses in the center of the dipolar evolution time to refocus the chemical shift interaction (*2*).

In this study, practical performances of REDOR and SFAM sequences representing two different recoupling schemes under the MAS condition are explored. These recoupling efficiencies are determined by varying resonance offsets for the irradiated nucleus and sample positions in the sample spinner. The essential settings of experimental parameters to give reliable and quantitative data in these methods are investigated. Observed dipolar recoupling efficiencies for both methods show a different response to the rf inhomogeneity. By comparing their practical performances, it is anticipated that a direction to develop new methods can be obtained.

[1] To whom correspondence should be addressed. Fax: 850-644-1366. E-mail: cross@magnet.fsu.edu.

1090-7807/01 $35.00

EXPERIMENTAL

Enriched [1-^{13}C, ^{15}N]glycine was purchased from Cambridge Isotope Laboratories (Andover, MA). The sample was mixed with natural abundance glycine at a ratio of 1 : 4 and then recrystallized (*13*) through slow evaporation of water without further purification. Such dilution effectively attenuates intermolecular dipolar interactions (*14–16*).

All NMR measurements were carried out at 25°C on a Bruker DMX-300 NMR spectrometer equipped with a triple resonance probe with a 7.0-mm o.d. spinner assembly. The Larmor frequencies for ^{1}H, ^{13}C, and ^{15}N were 300.12, 75.64, and 30.12 MHz, respectively. The XY-8 and XY-16 pulse sequences (*17*) for irradiation of ^{15}N nuclei were employed in the REDOR experiments as illustrated in Fig. 1 to compensate for the flip angle error, the off-resonance effect, and the fluctuation of the ^{1}H field. Crystalline samples of about 10 mg were first placed in the central portion of the 7.0-mm rotor with 1.0-mm thickness along the spinner axis. In this sample position, the π pulse lengths of 9.5 and 13.5 μs for ^{13}C and ^{15}N channel, respectively, were calibrated and the ^{1}H decoupling field used was measured to be 75 kHz. In SFAM experiments, a 40-kHz depth of rf modulation and a 40-kHz maximum offset were used for irradiation on the ^{15}N channel. The same π pulse lengths and ^{1}H decoupling field were used in both SFAM and REDOR experiments and directly applied to other sample positions without recalibrating the power settings. Proton decoupling was achieved by two-pulse phase modulation (*18*) in all experiments. Precise sample positioning was achieved via specially designed Teflon spacers with $\pm$0.2-mm precision along the axial direction of the sample tube. The number of data acquisitions was varied from 64 to 6400 depending upon the dipolar recoupling periods in order to obtain a reasonable signal-to-noise ratio. The sample spinning was controlled to 4000 $\pm$ 1.0 Hz by a Bruker MAS control unit. The dipolar dephased and full echo spectra were recorded at various $N_c T_r$ values ranging from 2 to 24 ms for both SFAM and REDOR, where N_c and T_r are the number of rotor cycles and the rotor period, respectively. The normalized dipolar dephased signal is defined as $S_r/S_0 =$ (dipolar dephased/full echo) so that the transverse relaxation effect is suppressed in the plot. The signal intensities were analyzed as a sum of the center and sideband intensities (*12, 14–16*). All simulation of REDOR curves were carried out using a FORTRAN 77 program by taking finite π pulse lengths into account (*12*) and all numerical simulations for SFAM were carried out with the GAMMA magnetic resonance simulation platform (*19*).

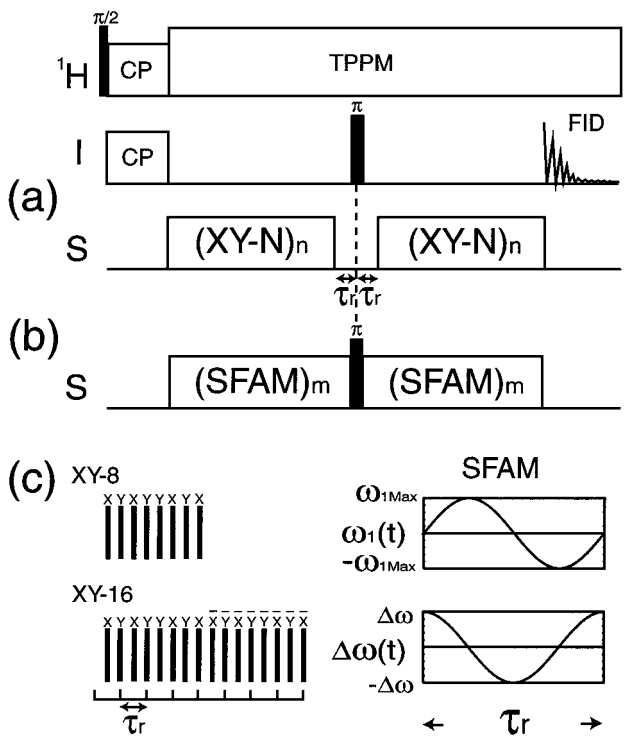

FIG. 1. Pulse sequences for rotational echo double resonance (REDOR) (a) and simultaneous frequency and amplitude modulation (SFAM) (b). Conventional cross polarization is used to prepare the initial magnetization for observed nuclei I (^{13}C). Proton decoupling was achieved by two-pulse phase modulation. (c) The continuous phase and amplitude modulated irradiation and XY-8, or 16 compensation-phase cycles, π pulse trains were applied to the unobserved nucleus in REDOR and SFAM experiments, respectively.

RESULTS AND DISCUSSION

rf Inhomogeneity in MAS Probe

Effects of rf inhomogeneity on important solid state NMR experiments have been previously published (*11, 12, 20*). However, in this study, quantitative estimates of spatially resolved rf inhomogeneity effects for distance measurements and a general strategy to characterize these effects are presented. Here "rf inhomogeneity" refers to a distribution of effective nutation fields dependent on sample position in a MAS spinner. In a CPMAS experiment with an inhomogenous rf environment for the sample, the observed signal intensity may vary due to many factors. The flip angle error of the ^{1}H excitation pulse and variation in net spin locking field during CP for both observed and ^{1}H nuclei are examples. Here, single pulse excitation with high power ^{1}H decoupling is more suitable for focusing on the flip angle errors of observed and irradiated nuclei due to the rf inhomogeneity.

Even the observed signal height based on one pulse excitation depends on both the flip angle change for the observed nucleus and the ^{1}H decoupling efficiency. Insufficient ^{1}H decoupling leads to line broadening, and therefore peak integration should be used.

The normalized peak integral at each site, I_i, within the spinner may be translated into a nutation frequency by using the equation (*21, 22*),

$$I_i = \left(\nu_{\mathrm{rf}}^{i}/\nu_{\mathrm{rf}}^{0}\right) * \sin\left[\left(2\pi * \nu_{\mathrm{rf}}^{i}\right) * t_{\mathrm{w}}\right], \qquad [1]$$

where ν_{rf}^{i} and t_{w} are the nutation frequency for each site and

pulse duration, respectively, and i indicates the sample position in the spinner. For the center of the spinner i equals 0.

In order to obtain quantitative peak integrals, we observed ^{13}C methyl signals from a rubber disk with high power ^{1}H decoupling using a fixed pulse length and without magic angle spinning. The methyl group in the rubber material gives rise to a relatively narrow ^{13}C signal due to large amplitude backbone and local motions and a small chemical shift anisotropy. A nutation experiment was carried out to measure the rf inhomogeneity of the full rotor, showing that the ratio of the intensities at the 450° and 90° nutation angles was 55.7% (plot not shown). A 1-mm thick rubber disk was positioned in the sample chamber along the MAS axis from the top to the bottom as illustrated in Fig. 2a for different experimental observations. Precisely speaking, the rf field is also radially inhomogeneous. For simplicity, an average rf nutation frequency is used to characterize the cylindrical segment occupied by the rubber disk. Figure 2b shows the profile of normalized ^{13}C methyl peak integrals. By using a weighted Gaussian curve to fit the profile, the center of the rf irradiation was determined to be 8.4 mm from the inner bottom of the sample tube. The peak integrals were translated into average nutation frequencies based on Eq. [1], whose profile is shown in Fig. 2c. The maximum average nutation frequency with the rf power used was 55.6 kHz. The average nutation frequency profile obtained is a bit broader than the signal intensity profile.

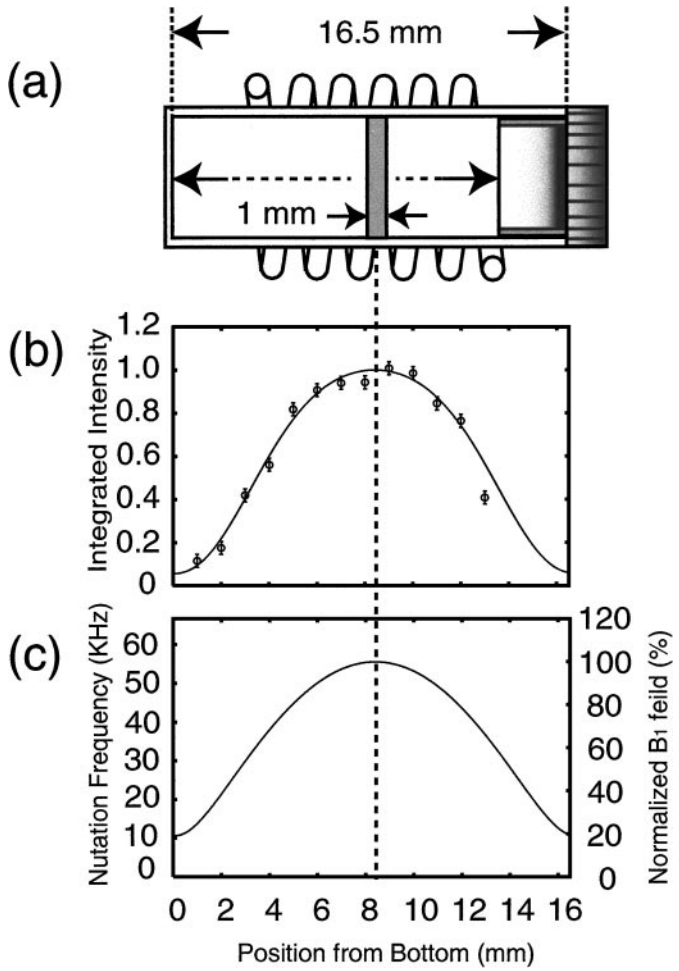

FIG. 2. (a) Schematic representation of 1.0-mm thickness rubber disk positioned within the Bruker 7-mm o.d. spinner with a solenoid coil. The coil length, i.d. and o.d. were 9.3, 7.3, and 8.5 mm, respectively. (b) The normalized ^{13}C methyl peak integrals at each position within the sample tube. (c) Position-dependent effective rf field variation profile translated from (b) based on Eq. [1]. Left and right axes are effective nutation frequency and normalized nutation frequency percentages.

Sample Position Dependence of Dipolar Recoupling Efficiency

For the dipolar recoupling experiment, relatively long mixing times must be used to assess the recoupling efficiency. However, the observed signal will be decreased significantly during long dipolar evolution times due to transverse relaxation (i.e., T_2). The sample positions for SFAM and REDOR experiments are redefined as illustrated in the column of Fig. 3 allowing us to use more samples in each position (2.4-mm thickness) for dipolar recoupling experiments. Because of the symmetric rf nutation frequency profile about the geometrical center of the spinner as shown in Fig. 2c, only positions 1 to 3 were observed (the experiment would be difficult to perform at sample position 4 due to low sensitivity). The average rf nutation frequency for each sample position 1, 2, and 3 were calculated as 97, 87, and 61%, respectively, based on the experimental rf nutation frequency profile shown in Fig. 2c.

In order to simulate the dephasing behavior at each position, only the dipolar coupling constant is changed to fit the experimental data without changing other parameters utilized in the experiment. The recoupling efficiency can be calculated as $(D_{\mathrm{IS}}^{\mathrm{obs}}/D_{\mathrm{IS}}) * 100$, where $D_{\mathrm{IS}}^{\mathrm{obs}}$ is the observed dipolar coupling constant through dipolar dephasing curve fitting and D_{IS} is the calculated dipolar coupling constant between the heteronuclear I and S spins. Figure 3 shows the experimental dipolar dephasing data from the SFAM and REDOR experiments superimposed by theoretical curves at different sample positions. Clearly the recoupling efficiency varies with the sample position for both SFAM and REDOR experiments. At position 1 the efficiency is nearly 100% for both experiments. Deviations of the experimental points from the theoretical curves in the oscillatory regions were observed for both experiments but were more pronounced for SFAM. The deviations could result from cross talk between the proton decoupling and the ^{15}N irradiation, if the ^{1}H decoupling amplitude is less than three times as large as that of the ^{15}N irradiation (*23, 24*). Compared to the REDOR measurements, SFAM is more sensitive to such cross talk because the ^{15}N channel irradiates throughout the time for dipolar dephasing. By using a lower ^{15}N irradiation amplitude to ensure that the ^{1}H decoupling amplitude is more than three times as large, such deviations are minimized, as shown in Fig. 4.

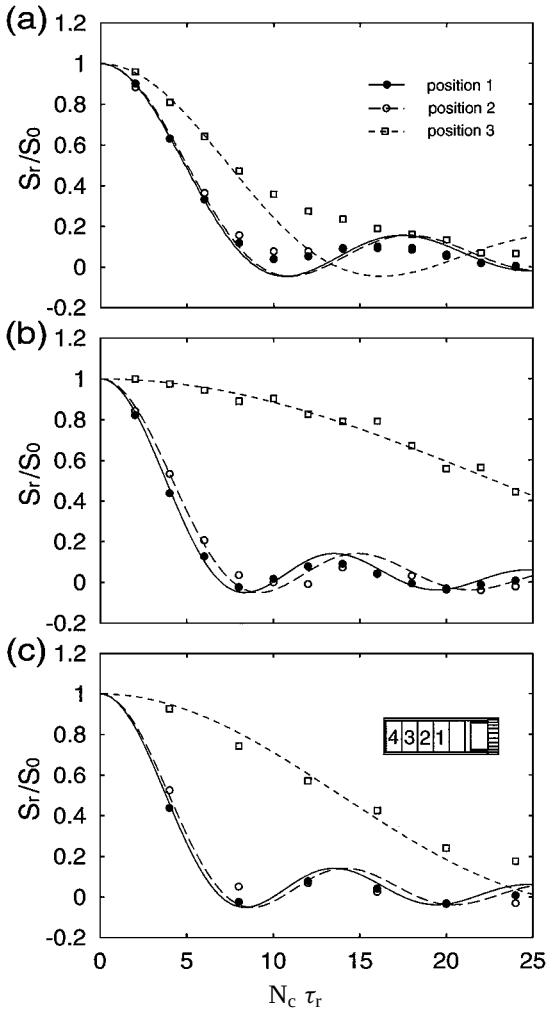

FIG. 3. Normalized dipolar dephased signal intensities with best fit theoretical curves for sample positions 1–3 for SFAM (a), REDOR with XY-8 (b), and with XY-16 (c)—sample position 1 (closed circle), position 2 (open circle), and position 3 (open square), respectively. MAS rate was set to 4 kHz for all experiments. Recoupling efficiency was 100.0, 97.62, and 65.89% for SFAM (a) for positions 1–3, respectively, and 100.0, 90.95, 16.74, and 100.0, 95.32, 27.36% for REDOR XY-8 (b) and XY-16 (c) for positions 1–3, respectively.

Recoupling efficiency of 98, 91, and 95% was obtained at position 2 for SFAM, REDOR XY-8, and XY-16, respectively. Clearly, the reduction of the recoupling efficiency is very subtle for SFAM but relatively large for the REDOR XY-8 sequence. The phase cycling of the REDOR XY-16 sequence partly compensates for the rf inhomogeneity effect resulting in a better recoupling efficiency compared to the XY-8 sequence. At position 3, a substantial reduction in the recoupling efficiency was observed for all experiments. In the REDOR experiments, although XY-16 compensated for the rf inhomogeneity effects somewhat better than XY-8, only 27 and 17% recoupling efficiencies were observed for XY-16 and XY-8, respectively. The dipolar dephasing curves fit the experimental data quite well even at such low recoupling efficiencies. In contrast, the recoupling efficiency for SFAM at sample position 3 was substantially better (66%). Once again the deviations between the experimental data and the theoretical curve near the oscillatory minimum were exaggerated because the proton decoupling at this sample position becomes much weaker, which could seriously compromise analysis efforts.

Irradiated Nuclear Carrier Frequency Offset Dependence

If the rf irradiation is applied to the isotropic resonance line (i.e., on-resonance), then the orientation dependent anisotropic resonances are under off-resonance irradiation. In MAS, the anisotropic chemical shift breaks up into a series of sidebands separated by the sample spinning frequency, if this frequency is not much larger than the size of the chemical shift anisotropy. Such spinning sidebands will continue to be a problem as large sample volumes and high magnetic fields are required. Even by using high spinning frequencies, the sidebands cannot be removed completely at high magnetic fields. This implies that the recoupling contribution from spinning sidebands may experience off-resonance irradiation. Thus it is important to address the recoupling efficiency at different carrier offsets for the three sample positions using both SFAM and REDOR experiments.

From the measurements, we found that the recoupling efficiency was almost independent of the carrier offset frequency for up to 10 kHz at sample positions 1 and 2, where the effective nutation frequencies were 97 and 87%, respectively. It is revealed that the XY-8 and XY-16 sequences in the REDOR experiments can effectively compensate for the rf offset as well as for the small rf inhomogeneity. For SFAM, the rf offset and rf inhomogeneity can be overcome through the frequency and amplitude modulation parameters. However, at sample position 3, where the effective nutation frequency was only about 61%, the recoupling efficiencies clearly depend upon the carrier offset, particularly for the REDOR experiments, as shown in Fig. 5. Table 1 shows the variation in the recoupling efficiencies of the

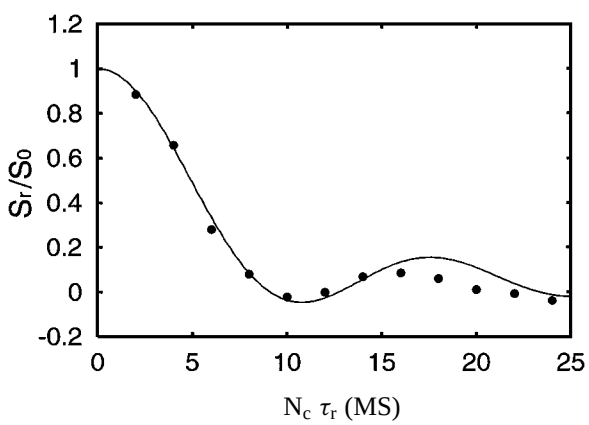

FIG. 4. Normalized dipolar dephased signal intensities with best fit theoretical curves at position 1 for SFAM. For SFAM the modulation frequency (ω_{1MAX}), and the maximum offset of the modulation ($\Delta\omega_{1MAX}$) were set to 25 kHz. ^{1}H decoupling amplitude was 75 kHz.

TABLE 1

The Comparison of Distribution of Recoupling Efficiency for Various Carrier Offset Frequencies with Respect to Those for On-Resonance Carrier Frequency at Sample Position 3

	The deviation (%)[a]		
	Carrier frequency offset (kHz)		
	2	5	10
SFAM	0	7.5	0.3
REDOR (XY-8)	64.7	35.3	57.1
(XY-16)	35.0	18.5	14.8

[a] Deviation $= ((R_{on} - R_i)/R_{on}) * 100$. R_{on}, dipolar recoupling efficiency for on resonance. R_i, dipolar recoupling efficiency for individual carrier offset frequencies.

SFAM and REDOR schemes at various carrier offsets with respect to on-resonance irradiation for the sample at position 3. It is clearly seen from Table 1 that the recoupling efficiency for SFAM is almost independent of the irradiation carrier frequency offset even if the effective nutation frequency is very low. On the other hand, the recoupling efficiency for REDOR with either the XY-8 or the XY-16 sequence strongly depends on the carrier offset under such a low effective nutation frequency, although the XY-16 sequence improves the recoupling performance by about a factor of 2 over the XY-8 sequence.

Overall Dipolar Recoupling Efficiency

Figure 6 shows the contour plots of the recoupling efficiencies for different schemes employed as a function of both the effective nutation frequency and the carrier offset. These contour plots were drawn based on the recoupling efficiencies experimentally obtained from 33 pairs of data sets (i.e., three sample positions and 11 different carrier offsets for each sample position), as described in the previous section. For each data set, 6 to 12 dipolar dephasing experiments (the pair of full echo and dipolar dephasing experiments) were used to determine the echo intensity changes with or without dipolar dephasing, as shown in Figs. 3 and 5. Thus, in total, over 708 experiments were performed for each contour plot.

It is illustrated in Fig. 6 that the profile for the recoupling efficiency strongly depends on the dipolar recoupling method employed. For SFAM, as shown in Fig. 6a, the recoupling efficiency gradually decreases as the effective rf nutation frequency decreases. A high recoupling efficiency (>95%) can be achieved when the effective nutation frequency is larger than 85%. Even when the effective nutation frequency is as low as 65%, over 70% recoupling efficiency can still be obtained. At a given effective nutation frequency, the variation in recoupling efficiency over the carrier offset is relatively small and a local maximum recoupling efficiency is observed at an offset of about 4 kHz. Therefore, the results imply that neither the recoupling efficiency for SFAM nor the carrier offset is sensitive to the rf field inhomogeneity, although no phase cycling is employed in the experiments. On the other hand, for REDOR, even with XY-8 and XY-16 phase cycling sequences, the recoupling efficiency is strongly dependent upon the effective nutation frequency, as shown in Fig. 6b and 6c. Both the XY-8 and XY-16 sequences exhibit a high recoupling efficiency (>95%) when the effective nutation frequency is larger than 92%. However, their recoupling efficiency decreases dramatically as the effective nutation frequency becomes less than 87%. With 65% effective nutation frequency, only about 40% recoupling efficiency is obtained. Therefore, it can be concluded that the recoupling efficiency for REDOR is very sensitive to the rf field inhomogeneity, even with the compensation phase cycling sequences. Compared to XY-8, the XY-16 sequence has slightly better recoupling efficiency at a given effective rf nutation frequency, especially for on-resonance irradiation. Furthermore, the XY-16 sequence exhibits a

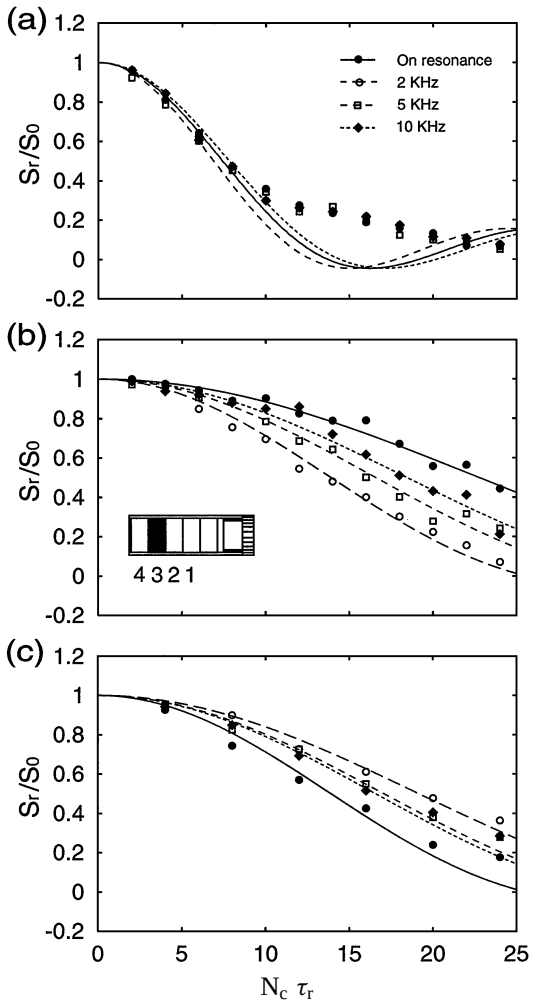

FIG. 5. Normalized dipolar dephased signal intensities with best fit theoretical curves for variation of carrier frequency offset for irradiated nuclei at position 3 for SFAM (a), REDOR with XY-8 (b), and with XY-16 (c), respectively. Carrier offset frequency was on-resonance (closed circle), 2 kHz (open circle), 5 kHz (open square), and 10 kHz off-resonance, respectively. Sample spinning rate was set to 4 kHz.

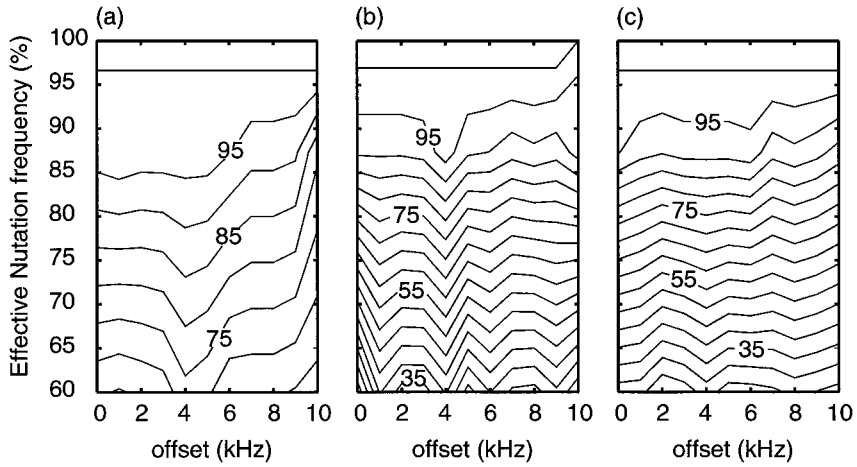

FIG. 6. The contour map of heteronuclear dipolar recoupling efficiency for rf inhomogeneity and carrier frequency offset of the irradiated nucleus for (a) SFAM, (b) REDOR with XY-8, and (c) with XY-16 compensation. The *z*-axis is the dipolar recoupling efficiency (%). All experiments were performed with three different sample positions and 11 different carrier offset frequencies. Each contour map is drawn based on experimentally obtained 33 pairs of carrier offset and sample positions—a total of 708 experiments for SFAM and REDOR with XY-8, and 450 for REDOR with XY-16.

relatively uniform recoupling efficiency versus the carrier offset for up to 10 kHz, while the XY-8 has a local maximum recoupling efficiency at an offset of 4 kHz, which is also observed in the SFAM measurements (c.f. Fig. 6a). Such a phenomenon can be understood as an interference of the heteronuclear dipolar recoupling with the chemical shift anisotropy that is partly recovered by the dipolar recoupling schemes, as previously reported by Ishii *et al.* (*4*).

CONCLUSION

Performances of the two different heteronuclear dipolar recoupling schemes, SFAM and REDOR, have been measured in the presence of well-defined rf inhomogeneity. It has been demonstrated here experimentally that SFAM is more tolerant of both the rf inhomogeneity and the carrier offset while REDOR, even with XY-8 and XY-16 phase cycling sequences designed for compensation of pulse imperfections, is relatively sensitive to the rf inhomogeneity and the carrier offset. A high recoupling efficiency (>95%) can be obtained for an effective rf nutation frequency greater than 85% for SFAM and greater than 92% for REDOR. Furthermore the recoupling efficiency decreases gradually for SFAM but drops sharply for REDOR as the effective rf nutation frequency decreases. Therefore, the continuous rf modulation scheme to recouple the dipolar interaction under MAS seems to have considerable advantages over the rectangular pulse scheme for insensitivity to rf inhomogeneity. From a practical point of view, some rf inhomogeneity across the sample coil is unavoidable, but it can be severe depending on the sample coil design and sample dimensions. Therefore, due to its tolerance of the rf inhomogeneity, the SFAM recoupling scheme not only allows one to use more sample in the measurements so that the sensitivity can be greatly enhanced, but also eliminates the effect of the instability of the NMR spectrometer, especially for long duration experiments. For the REDOR experiments, the samples have to be placed in a small area of the sample coil to ensure better rf field homogeneity to obtain accurate distance information. However, compared to REDOR, SFAM requires a much higher ^{1}H decoupling field during the recoupling period when continuous SFAM irradiation is used. Such irradiation may result in significant sample heating. For a dynamic sample such as a membrane protein, the heteronuclear dipolar coupling is partially averaged due to molecular motions. In such an environment, strong ^{1}H decoupling field may not need to be applied. So we can conclude that SFAM is suitable for such relatively mobile biological samples. On the other hand, REDOR is more suitable for relatively high sensitivity lipid biomolecular samples.

ACKNOWLEDGMENTS

The authors thank Dr. William Brey for useful discussion about the rf inhomogeneity. This research has been supported by National Science Foundation (MCB 99-86036) to TAC and the work was largely performed at the National High Magnetic Field Laboratory supported by the National Science Foundation Cooperative Agreement (DMR-9527035) and the State of Florida.

REFERENCES

1. T. Gullion and J. Schaefer, Rotaional-echo double-resonance NMR, *J. Magn. Reson.* **81,** 196–200 (1989).
2. R. Fu, S. A. Smith, and G. Bodenhausen, Recoupling of heteronuclear dipolar interactions in solid state magic-angle spinning NMR by simultaneous frequency and amplitude modulation, *Chem. Phys. Lett.* **272,** 361–369 (1997).
3. A. W. Hing, S. Vega, and J. Schaefer, Transferred-echo double-resonance NMR, *J. Magn. Reson.* **96,** 205–209 (1992).
4. Y. Ishii and T. Terao, Manipulation of nuclear spin Hamiltonians by rf-field modulations and its applications to observation of powder patterns under magic-angle spinning, *J. Chem. Phys.* **109,** 1–9 (1998).

5. D. P. Raleigh, M. H. Levitt, and R. G. Griffin, Rotational resonance in solid state NMR, *Chem. Phys. Lett.* **146,** 71–76 (1988).
6. T. Gullion and S. Vega, Simple magic angle spinning NMR experiment for the dephasing of rotational echoes of dipolar-coupled homonuclear spin pairs, *Chem. Phys. Lett.* **194,** 423–428 (1992).
7. R. Tycko and G. Dabbagh, Measurement of nuclear magnetic dipole–dipole couplings in magic angle spinning NMR, *Chem. Phys. Lett.* **173,** 461–465 (1990).
8. D. W. Gregory, D. J. Mitchell, J. A. Stringer, S. Kiihne, J. C. Shiels, J. Callahan, M. A. Mehta, and G. P. Drobny, Windowless dipolar recoupling: The detection of weak dipolar couplings between spin 1/2 nuclei with large chemical shift anisotropies, *Chem. Phys. Lett.* **246,** 654–663 (1995).
9. Y. K. Lee, N. D. Kurur, M. Helmle, O. G. Johnnessen, N. C. Nielsen, and M. H. Levitt, Efficient dipolar recoupling in the NMR of rotating solids. A sevenfold symmetric radiofrequency pulse sequence, *Chem. Phys. Lett.* **242,** 304–309 (1995).
10. P. R. Costa, B. Sun, and R. G. Griffin, Rotational resonance tickling: Accurate internuclear distance measurement in solids, *J. Am. Chem. Soc.* **119,** 10,821–10,830 (1997).
11. D. Horne, R. D. Kendrick, and C. S. Yannoni, Bond length measurements in amorphous solids by nutation NMR spectroscopy: The role of rf field homogeneity, *J. Magn. Reson.* **52,** 299–304 (1983).
12. A. Naito, K. Nishimura, S. Kimura, S. Tuzi, M. Aida, N. Yasuoka, and H. Saitô, Determination of the three-dimensional structure of a new crystalline form of N-Acetyl-Pro-Gly-Phe as revealed by ^{13}C REDOR, X-ray diffraction, and molecular dynamics calculation, *J. Phys. Chem.* **100,** 14,995–15,004 (1996).
13. B. P. Jonsson and A. Kvick, Precision neutron diffraction structure determination of protein and nucleic acid components. III. Crystal and molecular structure of amino acid a-glycine, *Acta Cryst.* **B28,** 1827–1833 (1972).
14. A. Naito, K. Nishimura, S. Tuzi, and H. Saitô, Inter- and intra-molecular contributions of neighboring dipolar pairs to the precise determination of interatomic distance in a simple [^{13}C, ^{15}N]-peptide by ^{13}C, ^{15}N-REDOR NMR spectroscopy, *Chem. Phys. Lett.* **229,** 506–511 (1994).
15. K. Nishimura, A. Naito, C. Hashimoto, M. Aida, S. Tuzi, and H. Saitô, Determination of the three-dimensional structure of crystalline Leu-enkephalin dihydrate based on six sets of accurately determined interatomic distances from ^{13}C-REDOR NMR and the conformation-dependent ^{13}C chemical shifts, *J. Phys. Chem. B* **102,** 7476–1783 (1998).
16. K. Nishimura, A. Naito, S. Tuzi, and H. Saito, Analysis of dipolar dephasing pattern in I-S_n multispin system for obtaining the information of molecular packing and its application to crystalline N-Acetyl-Pro-Gly-Phe by REDOR solid state NMR, *J. Phys. Chem.* **103,** 8398–8404 (1999).
17. T. Gullion, D. Baker, and M. S. Conradi, New, compensated Carr-Purcell sequences, *J. Magn. Reson.* **89,** 479–484 (1990).
18. A. E. Bennett, C. M. Rienstra, M. Auger, K. V. Lakshmi, and R. G. Griffin, Heteronuclear decoupling in rotating solids, *J. Chem. Phys.* **103,** 6951–6958 (1995).
19. S. A. Smith, T. O. Levante, B. H. Meier, and R. R. Ernst, Computer stimulations in magnetic resonance. An object-oriented programming approach, *J. Magn. Reson. Ser. A* **106,** 75–105 (1994).
20. G. C. Campbell, L. G. Galya, A. J. Beeler, and A. D. English, Effect of rf inhomogeneity upon quantitative solid-state NMR measurements, *J. Magn. Reson. Ser. A* **112,** 225–228 (1995).
21. S. Crozier, I. Brereton, F. O. Zelaya, W. U. Roffmann, and D. M. Doddrell, Sample-induced rf perturbations in high-field high-resolution NMR spectroscopy, *J. Magn. Reson.* **126,** 39–47 (1997).
22. W. W. Brey, "Rf Inhomogeneity in NMR Spectroscopy at High Field," 41st Experimental NMR Conference (2000).
23. W. P. Aue, D. J. Ruden, and R. G. Griffin, Uniform chemical-shift scaling—application to 2D resolved NMR-spectra of rotating powdered samples, *J. Chem. Phys.* **80,** 1729–1738 (1984).
24. Y. Ishii, J. Ashida, and T. Terao, ^{13}C-^{1}H dipolar recoupling dynamics in ^{13}C multipulse solid-state NMR, *Chem. Phys. Lett.* **246,** 439–445 (1995).